Formation and annihilation of stressed deformation twins in magnesium

Karim Louca[1*], Hamidreza Abdolvand[1*], Charles Mareau[2], Marta Majkut[3,4], Jonathan Wright[3]

[1]Department of Mechanical and Materials Engineering, Western University, London, Ontario, N6A 5B9, Canada

[2]Arts et Metiers ParisTech, Campus d'Angers, LAMPA, 2 Boulevard du Ronceray, 49035, Angers Cedex 1, France

[3]ESRF, 71 Avenue Des Martyrs, 38000 Grenoble, France

[4] AMVALOR Metz , Technopole METZ 2000, 4 rue Augustin Fresnel, 57070 Metz, France

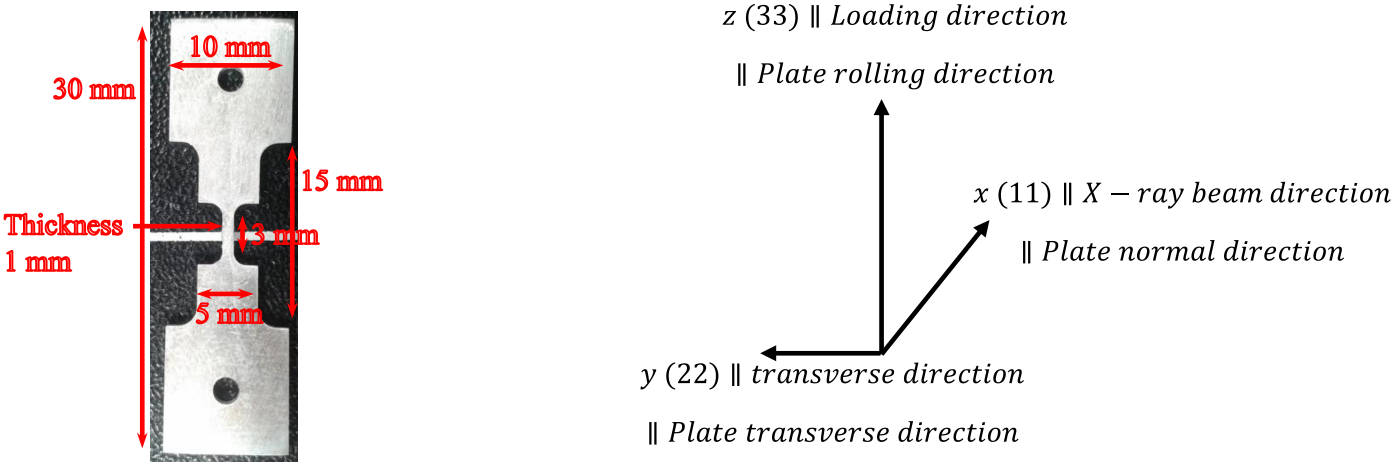

Supplementary Figure 1. The designed specimen and the coordinate systems of the experiment and the magnesium plate.

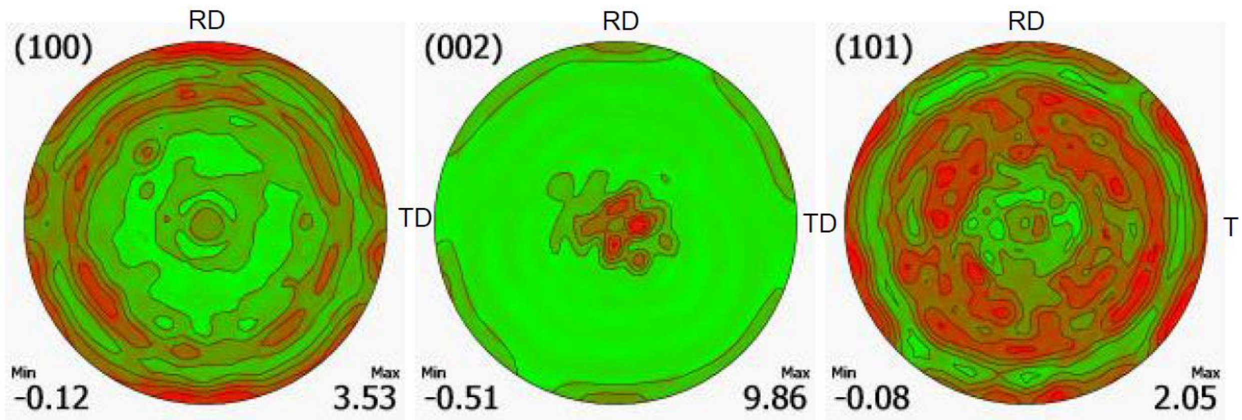

Supplementary Figure 2. Pole figures are measured using Lab XRD prior to 3D-XRD experiment. RD, ND, and TD represent Rolling, Normal, and Transverse direction of the magnesium plate.

Supplementary Table 1: Results of 3D-XRD experiment on Mg-2

Step	Step name	Applied strain %	Macroscopic stress (MPa)	No. of grains	Average No. Peaks per grain	Error in COM (μm)	Grain-weighted average stress with estimated errors (MPa)						Beam height (μm)
							σ_{11}	σ_{22}	σ_{33}	σ_{12}	σ_{13}	σ_{23}	
1	Preload	0.00	2	5542	141	±5.5	-5.9	-4.5	-3.6	1.5	0.0	-0.3	100
							±10.3	±7.1	±5.6	±3.4	±2.1	±2.4	
2	Onset-C	-0.0864	-42	5668	137	±5.5	-6.3	-2.7	-47.4	-1.8	0.7	0.6	
							±10.5	±7.1	±5.6	±3.4	±2.4	±2.1	
3	Plasticity-C1	-0.2919	-61	4038	117	±9.7	9.8	-2.1	-62.4	-2.7	1.5	-0.7	50
							±19.5	±12.9	±10.3	±6.3	±4.4	±3.9	
4	Plasticity-C2	-0.5	-70	1392	100	±12.1	9.7	-5.4	-58.8	-5.3	3.3	-2.5	25
							±26.0	±17.1	±13.8	±8.4	±5.9	±5.2	

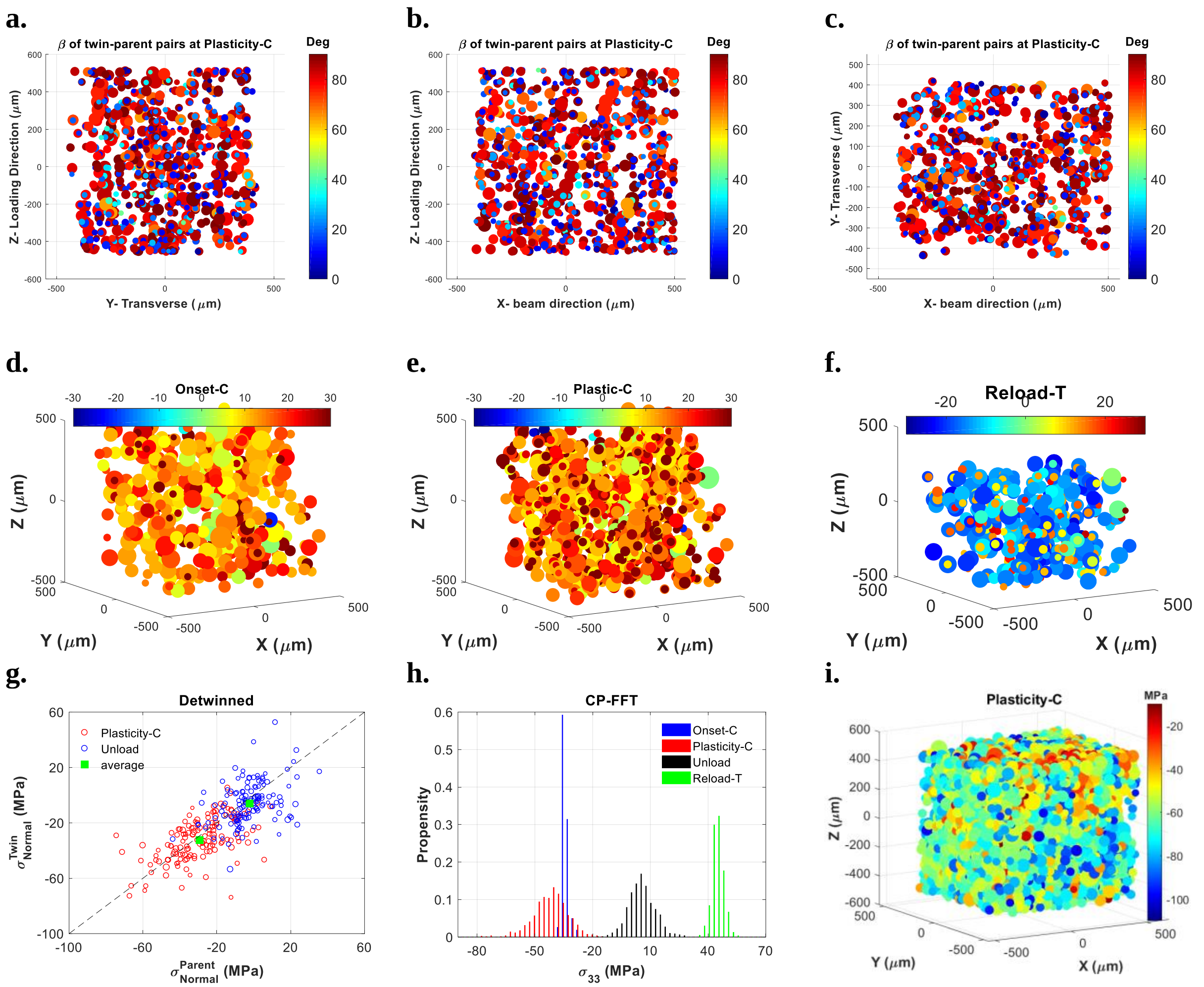

Supplementary Figure 3. The matched twin-parent pairs at the Plasticity-C: (a) Y-Z, (b) X-Z, and (c) X-Y projections. Grains are colour coded with respect to their β angle. A 3D map of the resolved shear stress acting on the twin habit plane from stresses measured in parents and those measured in twins at (d) Onset-C, (e) Plastic-C, and (f) Reload-T. (g) Measured stress normal to the twin habit plane for twins that detwinned. (h) Grain average stresses calculated using CP-FFT modelling. (i) Measured stresses along the loading direction at Plasticity-C. All results are for Mg-1.

Errors associated with elastic strains measured for twins and parents

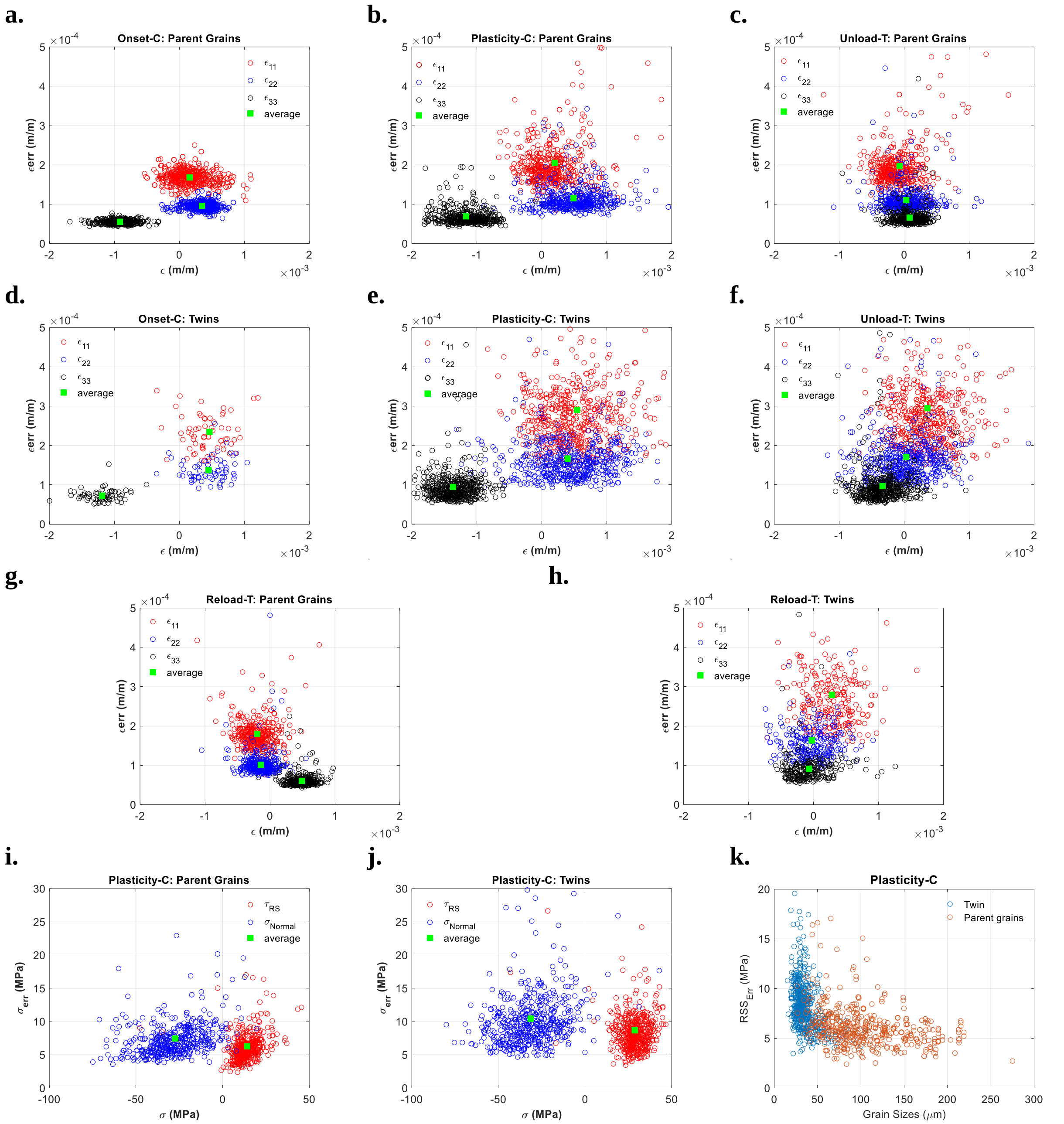

Supplementary Figure 4. Measured errors as a function of measured elastic axial strains for (a,b,c,g) parent grains and (d, e, f, h) their associated twins. Measured errors for twin resolved shear stress and stress normal to the twin habit plane for (i) parents and (j) twins. (k) The measured errors for twin resolved shear stress as a function of twin/parent grain size assuming that grains are spherical.

Supplementary Table 2: CP-FFT results

Steps	$\tau_{RS\,/\,Parent}$ [MPa]	$\tau_{RS\,/\,Twin}$ [MPa]	$\sigma_{n\,/\,Parent}$ [MPa]	$\sigma_{n\,/\,Twin}$ [MPa]	$\sigma_{33\,/\,Parent}$ [MPa]	$\sigma_{33\,/\,Twin}$ [MPa]
Onset-C	17	23	-17	-17	-34	-40
Plasticity- C	21	21	-27	-28	-47	-47
Unload	-3	-2	8	7	11	9
Reload-T	23	23	23	23	52	53

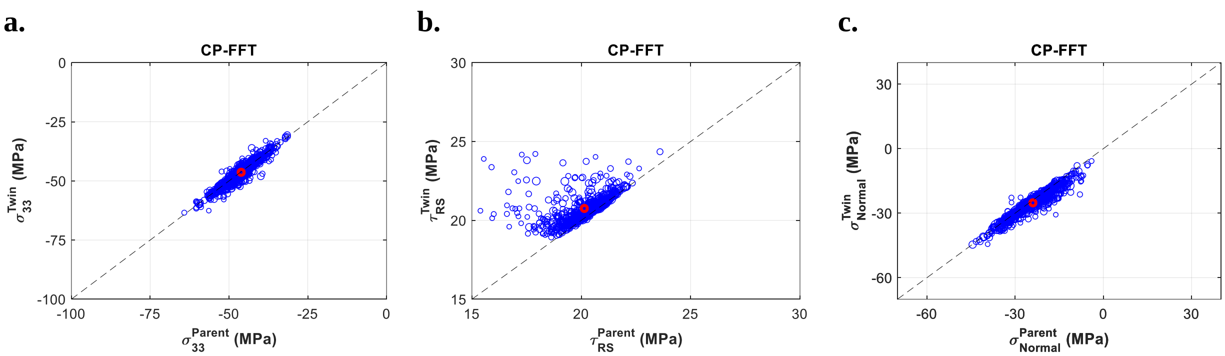

Supplementary Figure 5. An example of the CP-FFT results for stress in twin and parent pairs. All results are for Plasticity-C**.**

An example of a diffraction peak from a twin

To show how the size of the twin varies with stress in the twin and parent, a diffraction peak from a twin is shown in Fig 6. Fig. S6b-d show the $(1\bar{1}03)$ diffraction peak of a twin from Onset-C to Reload-T. In Fig. 6a the change in $\delta\tau_{RS}$ is shown where:

$$\delta\tau_{RS} = \tau_{RS}^{T} - \tau_{RS}^{P}$$

Fig. 6a shows a reduction in $\delta\tau_{RS}$ from onset to plasticity. The intensity and size of the diffraction peak increases from Onset-C to Plasticity-C indicating the increase in the size of the twin (Fig. 6c). Upon unloading and reloading, $\delta\tau_{RS}$ increases and the twin size is reduced as shown in Fig. 6d.

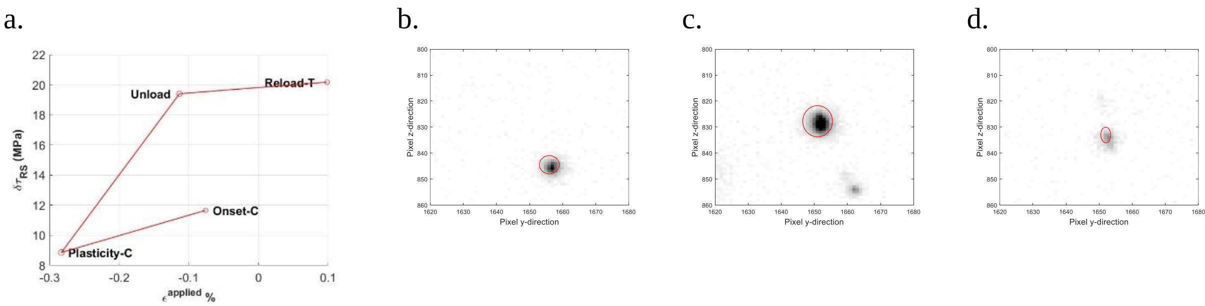

Supplementary Figure 6. (a) The evolution of $\delta\tau_{RS}$ in a twin-parent pair. Diffraction peaks from $(1\bar{1}03)$ plane of a twin at (b) Onset-C, (c) Plasticity-C, and (d) Reload-T**.**

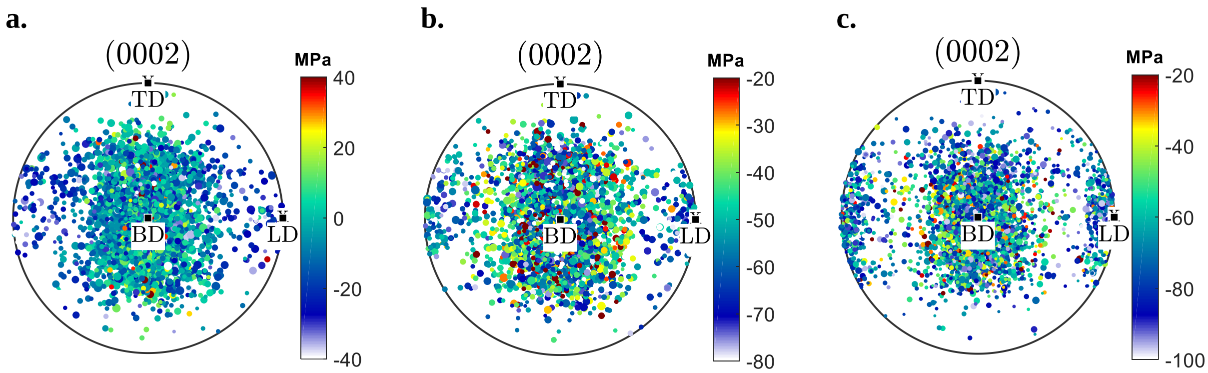

Supplementary Figure 7. The measured (0002) pole figures for the Mg-2 sample at (a) preload, (b) Onset-C, and (d) Plasticity-C1 steps. Grains are colour coded with respect to their stresses in the loading direction (LD) and the size of each circle is proportional to the measured relative volume for the grain.

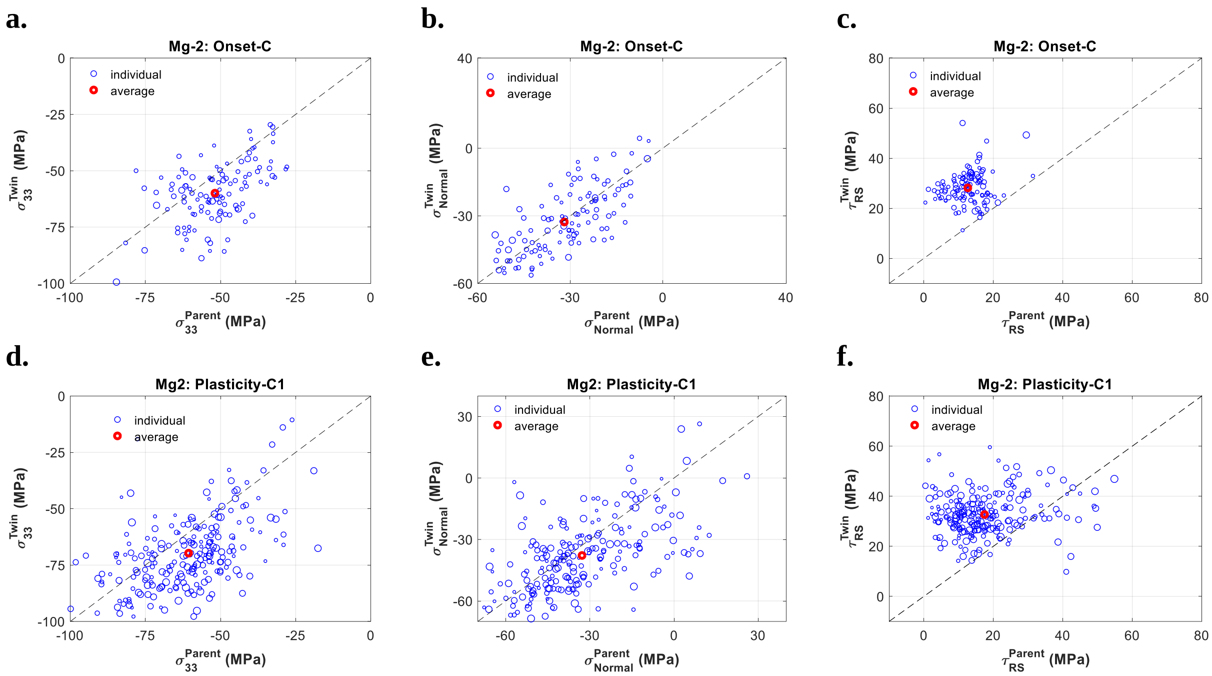

Supplementary Figure 8. Formation of twins in Mg-2: Measured σ_{33} in twins as a function of measured σ_{33} in the corresponding parents for (a) Onset-C and (d) Plasticity-C1. Measured stress normal to the twin habit plane for twins as a function of those measured for parents at (b) Onset-C and (e) Plasticity-C1. Measured resolved shear stress on the twin habit plane in the twinning direction for twins and parent pairs at (c) Onset-C and (f) Plasticity-C1.

Grain neighbourhood effects

Understanding and characterizing neighbourhood effects on twinning in 3D is not straightforward specially when the actual gain boundaries or twin boundary intersections are not known. Following is a brief summary of the conducted grain neighbourhood analysis.

Using the COMs and volumes of the indexed grains, a weighted Voronoi grain map is reconstructed to determine grain boundaries and identify neighbours of all grains in 3D. The twins nucleated in the third step (Plastic-C) are studied here. The effects of basal and prism slip transfer on the nucleation of a twin are investigated. A compatibility factor is used for every basal and prism slip system in neighbouring grains:

$$m = (n_s . n_t)(b_s . b_t)$$

where n_s and n_t are the unit vectors normal to the slip and twinning planes, and b_s and b_t are the normalized burger vectors of the slip and twinning planes respectively. When m is equal to 1, the twin variant and its neighbouring slip system are aligned. In addition, in order to determine if a slip system is active, resolved shear stresses are calculated on all slip systems and are compared against their corresponding CRSS values, i.e. 5 MPa for slip on basal systems and 25 MPa for slip on prism systems. In order to have a twin nucleation event via slip transfer, the neighbouring slip system must be activated prior to twin nucleation. Hence, the resolved shear stress acting on the active slip system should be close to its CRSS. As such, for the twins that nucleate at Plasticity-C, the following condition was used for the slip systems in the neighbouring grains at Onset-C:

$$\tau_{RS}^{Onset-C} > 0.9\tau^{CRSS}$$

where $\tau_{RS}^{Onset-C}$ is the RSS of the slip system in the neighbouring grain at Onset-C and τ^{CRSS} is the CRSS of the same slip system. This criterion is checked for all slip systems in all neighbours of a twinned parent grain while the active slip system with the highest compatibility factor is recorded. Fig. 9 shows the variation of the highest compatibility factor of the neighbouring basal slip systems as a function of the twin Schmid factor (SF) of the identified parent grains. If slip transfer mechanism was active, a decreasing trend would have been seen where twins with low SFs were nucleated due to activity of slip in the neighbouring grain. While a few low SF twins have high compatibility factors with slip on basal planes, a concrete conclusion cannot be made from the data. This mechanism occurs at the scale smaller than the one used in 3D-XRD experiment and higher resolution techniques are required to further investigate such mechanisms. In addition, no correlation was observed between twin nucleation and slip activity on the prism planes in the neighbouring grains. This is due to the fact that the applied stress was not high enough to cause substantial slip activity on the prism planes. That is, the condition in the above equation was not satisfied.

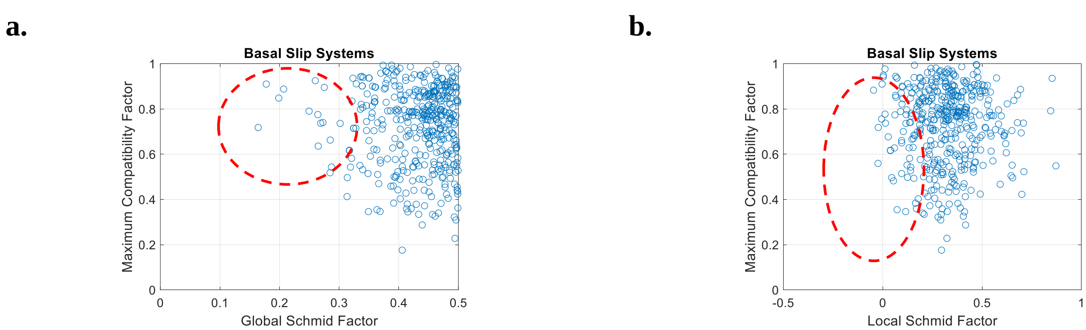

Supplementary Figure 9. Calculated maximum compatibility factor as a function of (a) global and (b) local Schmid factors for basal slip systems.

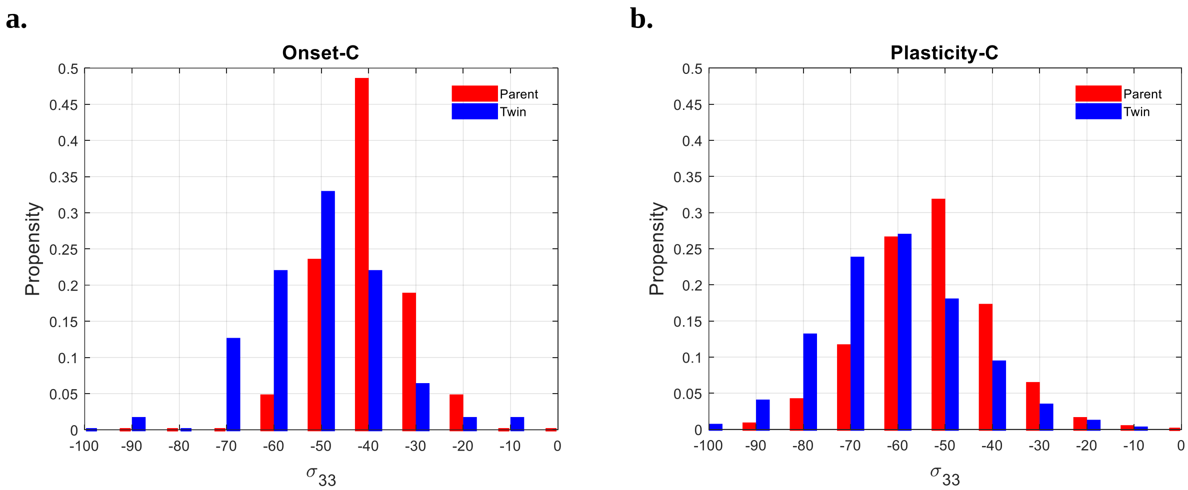

Supplementary Figure 10. Distribution of σ_{33} in twins and parent grains at (a) Onset-C and (b) Plasticity-C.

Calibration of single crystal parameters

a.

Ring Number	**Plane - hkl**	**Diffraction Angle (2θ)**	**Peaks per ring**
1	(100)	5.09°	76665
2	(101)	5.76°	117460
3	(102)	7.44°	79982
4	$(2\bar{1}0)$	8.81°	78000
5	(103)	9.60°	59355
6	(200)	10.18°	50678
7	$(2\bar{1}2)$	10.35°	51269
8	(201)	10.54°	104842
9	(202)	11.54°	91901
10	(104)	12.00°	30495
11	(203)	13.05°	86132
12	$(3\bar{1}0)$	13.48°	80553
13	$(3\bar{1}1)$	13.75°	210235
14	$(2\bar{1}4)$	14.00°	51217

b.

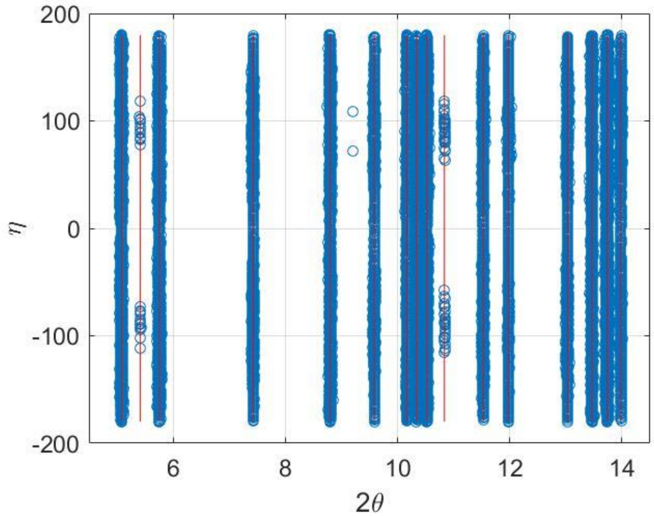

Supplementary Figure 11. (a) An example of the indexed planes at the preload: diffraction spots and their corresponding diffraction angles. (b) $\eta - 2\theta$ plot of the diffraction rings. η is the clock position of the diffraction spot on the diffraction pattern, and 2θ is the radial position.

Peaks assigned to each grain are used to determine 12 grain properties: 3 grain positions, 3 orientations, and 6 strain components or lattice parameters (a, b, c, α, β, γ). From the measured peaks, strains are calculated for individual grains as,

$$\epsilon_i = \frac{1}{2}\left(A_i A_0^{-1} + (A_i A_0^{-1})^T\right) - I$$

Where the grain specific metric, A_i is defined as,

$$A_i = \begin{bmatrix} a_i & b_i \cos(\gamma_i) & c_i \cos(\beta_i) \\ 0 & b_i \sin(\gamma_i) & -c_i \sin(\beta_i)\cos(\alpha_i^*) \\ 0 & 0 & c_i \sin(\beta_i)\sin(\alpha_i^*) \end{bmatrix}$$

where a_i, b_i, c_i, α_i, β_i, and γ_i are the lattice parameters estimated based on the positions of the peaks assigned to each grain. A_0 (or d_0) is the lattice parameters of the HCP crystal under no load, i.e. the reference lattice parameters.

At the preload, a set of initial parameters are defined to calculate strains for individual grains. The weighted average of the corresponding stress is then calculated and used for adjusting the "stress-free" lattice parameters. This procedure was conducted for the first, last and the middle two layers of the entire probed volume at the preload, i.e. 4 layers out of 10 are used for determining A_0. An average of the acquired lattice parameters from the four layers is then used for calculating strains across the all 10 layers. When the stress from all layers are equal to the applied stress, the initial lattice parameters are considered converged. These parameters are fitted using four layers but works on all 10 layers as proof of convergence. The fitted parameters for preload are used for all other loading steps to determine stress within individual grain.